

# Black Carbon aerosol measurements and simulation in two cities in south-west Spain

C. Milford<sup>a,b</sup>, R. Fernández-Camacho<sup>a</sup>, A. M. Sánchez de la Campa<sup>a</sup>, S. Rodríguez<sup>b</sup>, N. Castell<sup>c</sup>, C. Marrero<sup>b</sup>, J. J. Bustos<sup>b</sup>, J. de la Rosa<sup>a</sup> and A.F. Stein<sup>d</sup>

<sup>a</sup>Centre for Research in Sustainable Chemistry (CIQSO), Joint Research Unit to CSIC “Atmospheric Pollution”, University of Huelva, Huelva, Spain

<sup>b</sup>Izaña Atmospheric Research Center, AEMET, Joint Research Unit to CSIC “Studies on Atmospheric Pollution”, Santa Cruz de Tenerife, Canary Islands, Spain

<sup>c</sup>NILU-Norwegian Institute for Air Research, PO Box 100, NO-2027 Kjeller, Norway

<sup>d</sup>Air Resources Laboratory, National Oceanic and Atmospheric Administration, College Park, Maryland, USA

Correspondence to: C. Milford (cmilford@aemet.es)

## Abstract

Black carbon (BC) has been simulated for south-west Spain with the air quality model CAMx driven by the MM5 meteorological model, with a spatial resolution of 2 km x 2 km and a temporal resolution of 1 h. The simulation results were evaluated against hourly equivalent black carbon (EBC) concentrations obtained in the cities of Seville and Huelva for a winter period (January 2013) and a summer period (June 2013). A large seasonal variability was observed in PM<sub>2.5</sub> EBC concentration in the two cities, with higher concentrations in wintertime; summertime EBC concentrations were typically less than half those of the wintertime. The model captured the large diurnal, seasonal and day to day variability in these urban areas, mean biases ranged between -0.14 to 0.07  $\mu\text{g m}^{-3}$  in winter and between 0.01 to 0.29  $\mu\text{g m}^{-3}$  in summer while hourly PM<sub>2.5</sub> EBC observations ranged between 0.03  $\mu\text{g m}^{-3}$  to 10.9  $\mu\text{g m}^{-3}$ . The diurnal variation in EBC concentrations was bimodal, with a morning and evening peak. However, the EBC evening peak was much smaller in summer than in winter. The modelling analysis demonstrates that the seasonal and day to day variability in EBC concentration in these urban areas is primarily driven by the variation in meteorological conditions. An evaluation of the role of regional versus local contributions to EBC

30 concentrations indicates that in the medium size city of Seville, local on-road sources are  
31 dominant, whereas in the small size city of Huelva, local as well as regional sources produce a  
32 similar contribution. Considering the large diesel share of the vehicle fleet in Spain (currently  
33 ~ 56%), we conclude that continued reduction of BC from diesel on-road sources in these  
34 urban areas is indeed a priority, and we suggest that targeted mitigation strategies, for  
35 example reducing the heaviest emitters in wintertime, would yield the greatest benefits.

36 **Keywords:** Black Carbon, Air Quality, CAMx, Model Evaluation

## 37 **1 Introduction**

38 Black carbon (BC) has been identified as one of three key short-lived climate pollutants  
39 (SLCPs) for which emission reduction measures could contribute to slowing near-term  
40 climate change while having the co-benefit of improving air quality and thereby reducing the  
41 adverse health effects of air pollution (UNEP, 2011). Bond et al. (2013) concluded that the  
42 total black carbon climate forcing (including direct, indirect and snow and ice effects) is  
43 positive and is second only to carbon dioxide in terms of its climate forcing in our present day  
44 atmosphere. The potential for climate change mitigation through BC emission reductions  
45 depends on geographical region and is source dependent as co-emissions of organic carbon,  
46 sulphate and gaseous species affect the net climate forcing. Bond et al. (2013) suggest that  
47 diesel sources provide the most promising black carbon mitigation options due both to their  
48 positive net climate forcing and to the availability of abatement technologies and their  
49 implementation potential.

50 The adverse health effects of particulate matter (PM) are well known and documented (e.g.  
51 Brook et al., 2010; Lepeule et al., 2012; Pope et al., 2009; WHO, 2013). A recent extensive  
52 review of the health effects of black carbon (WHO, 2012) concluded that there is sufficient  
53 evidence of adverse effects of BC exposure and suggested that BC, although in itself may not  
54 be a major toxic component of PM<sub>2.5</sub>, may act as a universal carrier of toxic components to  
55 the body. Furthermore, the International Agency for Research on Cancer (IARC) recently  
56 classified diesel engine exhaust as carcinogenic to humans (IARC, 2012). In addition, BC has  
57 been identified as a more sensitive indicator to vehicle exhaust related air pollution compared  
58 with measurements of PM mass such as PM<sub>10</sub> and PM<sub>2.5</sub> (e.g. Janssen et al., 2011; Keuken et  
59 al., 2012). Reche et al. (2011) recommended the measurement of BC at air quality monitoring  
60 sites alongside measurements of PM mass and particle number concentration, to more fully  
61 reflect the impact of vehicle exhaust emissions on ambient air quality.

62 There have been various global (e.g Koch et al., 2009; Gilardoni et al., 2011) and regional  
63 modelling studies of BC or elemental carbon (EC) (e.g. Schaap, 2004; Simpson et al., 2007;  
64 Tsyro et al., 2007; Genberg et al., 2013; Hienola et al., 2013). However, modelling studies  
65 focussing on the mesoscale are scarcer. Sciare et al. (2010) modelled inorganic and  
66 carbonaceous aerosols and their relative contribution to  $PM_{2.5}$  mass in the Paris area while  
67 Couvidat et al. (2013) modelled elemental carbon and organic carbon (OC) also in the Paris  
68 area. In general, both studies reported a satisfactory performance for EC with Couvidat et al.  
69 (2013) observing both over and under-estimation of EC depending on the measurement site  
70 and measuring period. Ensberg et al. (2013) conducted a modelling study of black carbon and  
71 inorganic aerosols in the Los Angeles Basin and reported that BC predictions were generally  
72 in good agreement with the measurements at their ground site although the model did miss  
73 peak concentrations on specific days. These urban studies were conducted during spring or  
74 summer periods. Keuken et al. (2013) report a modelling study of EC at regional, urban and  
75 traffic sites in The Netherlands for 2011 and found that the model overestimated  
76 concentrations at regional sites and at urban background sites, likely due to too high primary  
77  $PM_{2.5}$  emissions and/or EC fractions and a too low road traffic emission height. They found  
78 good agreement between their modelled and measured traffic contribution to EC.

79 A limitation in the evaluation of modelling studies of BC is the availability of high quality  
80 measurements, particularly as monitoring of BC in ambient air at urban sites is, up to this  
81 date, not required by EU legislation (EEA, 2013) and so is not frequently measured. In light  
82 of these aspects, a BC measurement program with high temporal resolution was initiated in  
83 two cities in south-west Spain in 2012 to characterise the behaviour of this species. In  
84 addition to the measurement program, a three-dimensional air quality model (CAMx) was  
85 implemented to investigate the dynamics of this primary aerosol and its spatial and temporal  
86 variability and to explore the controlling factors on the BC concentrations in these urban  
87 areas. This study presents measurements and simulation of BC for a winter period (January  
88 2013) and a summer period (June 2013) from this measurement dataset. The structure of the  
89 paper is as follows, Section 2 describes the measurements and model set up, Section 3  
90 includes results and discussion of the evaluation of the model simulations on a seasonal and  
91 diurnal scale and an assessment of regional versus local sources, while conclusions are  
92 presented in Section 4.

## 93 **2 Methodology**

### 94 **2.1 Measurements**

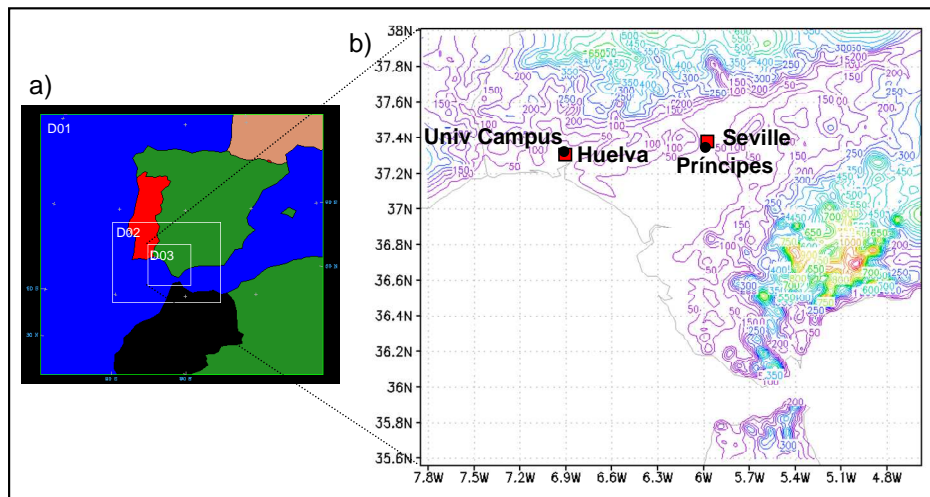
95 Black Carbon was measured, simultaneously, at two urban sites in the cities of Seville  
96 (~700,000 inhabitants) and Huelva (~150,000 inhabitants), in the south-west of Spain.  
97 Optical measurements of black carbon in PM<sub>10</sub> were conducted with a Multi-Angle  
98 Absorption Photometer (Thermo™, model CARUSSO 5012) measured with a ten-minute  
99 resolution (subsequently averaged to hourly resolution). The instrument set up is described in  
100 Fernández-Camacho et al. (2010). These were converted to equivalent black carbon (EBC)  
101 mass concentrations for each site by comparing with PM<sub>10</sub> filter samples (quartz-fibre,  
102 MUNKTELL™) collected in a high volume Graseby Anderson™ sampler (68 m<sup>3</sup> h<sup>-1</sup>)  
103 analysed for elemental carbon (EC) in the laboratory using the Thermo Optical Transmittance  
104 technique with a Sunset Laboratory™ OC-EC analyser and the EUSAAR2 (European  
105 Supersites for Atmospheric Aerosol Research) protocol (Cavalli et al., 2010). The term  
106 equivalent black carbon is used hereafter for the measurements reported here, following  
107 recommendations on Black Carbon terminology by the GAW Aerosol Scientific Advisory  
108 Group (GAW/WMO, 2011) and Petzold et al. (2013). The site specific mass-absorption  
109 efficiencies (MAE) obtained were 9.79 and 10.31 m<sup>2</sup> g<sup>-1</sup> for Seville and Huelva, respectively.  
110 The mean measured PM<sub>2.5</sub>/PM<sub>10</sub> BC ratio (0.74 ± 0.025) was utilised to determine the PM<sub>2.5</sub>  
111 BC concentration (see Fernández-Camacho et al., 2010 for more details).

112 The measurement sites used were (see Fig. 1):

- 113 • Príncipes (37.375° N, 6.006° W, 8 m a.s.l.), an urban background site influenced by road  
114 traffic located in a park in the south-west of the city of Seville. The closest roads lie about  
115 50 m to the east and 65 m to the north-west of the measurement site.
- 116 • University Campus (37.272° N, 6.925° W, 17 m a.s.l.), an urban background site located on  
117 the north-east side of the city of Huelva. There are some minor roads within the university  
118 campus, aside from these, the closest roads lie within about 150 m to 250 m of the  
119 measurement site.

120 The measurements were conducted in Seville for a period of 18 months (June 2012 to  
121 November 2013) and in Huelva for a period of 12 months (December 2012 to November  
122 2013). In this study, we present measurements and simulation of EBC for January and June  
123 2013.

124 In addition, the meteorological simulations that determine the transport and dispersion of BC  
125 were compared against surface-based observational data from 12 meteorological stations,  
126 belonging to the Meteorological State Agency of Spain (AEMET). The measurements used to  
127 evaluate the meteorological simulations were hourly measurements of wind speed and wind  
128 direction at 10 m, air temperature at 2 m, and precipitation. Road-traffic intensity (number of  
129 vehicles per hour) was also measured on the main road (Avenida de Blas Infante) close to the  
130 Príncipes measurement site in Seville.



131  
132 Figure 1. a) Map of the three model domains (D01, D02 and D03) and b) terrain height (m a.s.l.) of the inner  
133 domain (D03). Also shown are the locations of the measurement sites, Príncipes, Seville and University Campus,  
134 Huelva.

## 135 2.2 Model Description and Set Up

136 The air quality model chosen for this study was the Comprehensive Air-quality Model with  
137 eXtensions (CAMx) version 4.51 (ENVIRON, 2008). CAMx is a three-dimensional Eulerian  
138 chemistry transport model including aerosol chemistry. In this study we used the CF aerosol  
139 scheme. Three nested domains were used in the CAMx simulations, with 18 x 18 km, 6 x 6  
140 km and 2 x 2 km horizontal resolution. The outer domain (D01) covers the Iberian Peninsula,  
141 and parts of southern France and North Africa; domain (D02) includes southern Spain and  
142 southern Portugal while the inner domain (D03) covers the study area, the south-west region  
143 of Spain (see Fig. 1).

144 Initial and boundary conditions for the modelling outer domain were taken from the GEOS-  
145 Chem global transport model (Bey et al., 2001; Barrett et al., 2012). The GEOS-Chem model  
146 output was for the year 2006, monthly average values were generated for January and June to

147 use as input for our simulation. A spin-up of 72 h was carried out prior to each CAMx  
148 simulation to minimize the sensitivity of the results to the initial conditions.

149 Meteorological input data for the CAMx simulations were provided by the non-hydrostatic  
150 Mesoscale Meteorological model (MM5) v3.7 (Grell et al., 1995). Three grids (using two-way  
151 nesting) with the same horizontal resolution of 18, 6 and 2 km were used. MM5 was  
152 configured with 30 vertical layers in a terrain following coordinate system, with increasing  
153 vertical resolution closer to the surface. The model top corresponds to approximately 550hPa  
154 with a surface layer of about 35 m above ground. CAMx was run with 16 of the first 18  
155 vertical layers utilised in MM5. The European Centre for Medium-range Weather Forecasts  
156 (ECMWF) numerical weather prediction model analysis provided initial and boundary  
157 conditions for MM5 at six hourly intervals with a resolution of 0.25°.

### 158 **2.3 Emissions**

159 The emission inventory used in this study was based on Castell et al. (2010) and Milford et al.  
160 (2013). The outer domains include anthropogenic emissions from the European Monitoring  
161 and Evaluation Program (EMEP) emission inventory for the reporting year 2012  
162 (<http://www.emep.int>) interpolated to 18 km and 6 km spatial resolution. The inner domain  
163 includes industrial emissions, from both area and point sources, and on-road traffic emissions.

164 Industrial emissions in the inner domain were taken directly from the Spanish Pollutant  
165 Release and Transfer Register (PRTR-E; <http://www.prtr-es.es>) for the year 2013. This  
166 register contains emissions from all large industrial installations and these emissions were  
167 then separated into area and point sources. Particulate emissions in this register are given as  
168 PM<sub>10</sub>. PM<sub>2.5</sub> emissions were estimated for each industrial installation using source dependent  
169 PM<sub>2.5</sub>/PM<sub>10</sub> fractions (CEIDARS, 2012). PEC (Primary Elemental Carbon) emissions were  
170 derived from PM<sub>2.5</sub> emissions utilising mass fractions assigned to different source profiles  
171 (EPA, 2009).

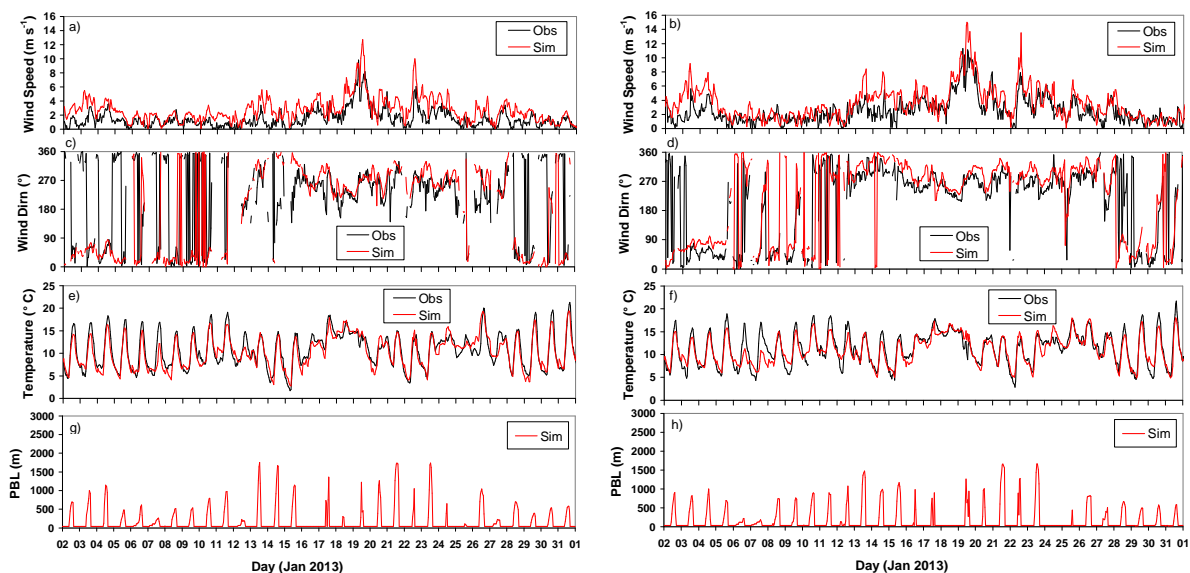
172 The on-road traffic emissions were obtained from the Spanish National Emission Inventory  
173 for the year 2011, as this was the most recent data available at the time of the study. These  
174 emissions were spatially disaggregated using the road network distribution in the study region  
175 and the average traffic intensity across that network. An hourly temporal profile differing for  
176 workdays and weekends was used for the temporal disaggregation of the emissions (Castell et  
177 al., 2010). Chemical speciation of primary PM<sub>2.5</sub> emissions for on-road traffic into PEC  
178 emissions was also conducted using source dependent mass fractions (EPA, 2009).

179 Residential combustion emissions are not currently included in the emission inventory for the  
180 inner domain.

### 181 3 Results and Discussion

#### 182 3.1 Meteorology

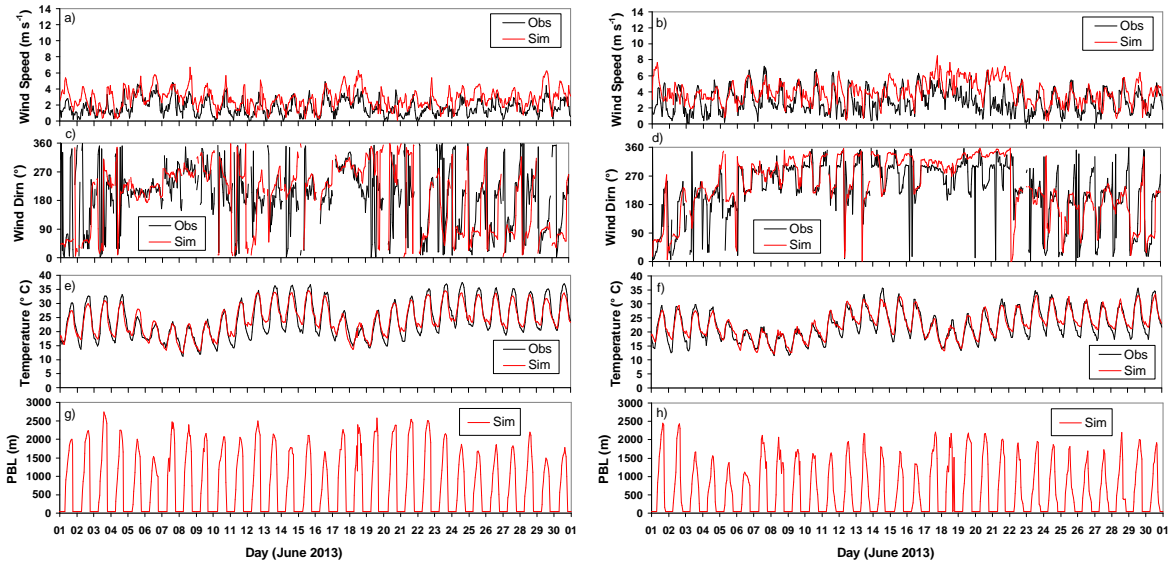
183 The evaluation of the meteorological simulations against surface-based observational data  
184 showed that the model captured most of the seasonal, diurnal and spatial variability. The  
185 meteorological stations located closest to the measurement sites were Seville Tablada (located  
186 about 1 km south from Príncipes, Seville) and Ronda Este (located about 2 km north-east  
187 from University Campus, Huelva). Observed and simulated wind speed, wind direction, and  
188 temperature data are shown in Fig 2 and Fig. 3 for the Seville Tablada and Ronda Este sites  
189 for the winter (January) and summer (June) simulations, respectively.



190  
191 Figure 2. Observed and simulated wind speed (a, b) and wind direction (c, d) at 10 m, temperature at 2 m (e, f)  
192 and simulated PBL height (g, h) during January 2013 at Seville Tablada (left panel) and Ronda Este (right  
193 panel).

194 The meteorological model had a tendency to overpredict the wind speed at both the Seville  
195 and Huelva sites; mean wind speed biases were similar during the winter and summer periods  
196 for both sites and ranged from 0.9 to 1.1 m s<sup>-1</sup> (Table 1). The mean biases in simulated 2 m  
197 temperature were low for both sites, with values ranging from -0.4 °C in winter to 0.4 °C for  
198 the summer period (Table 1). The simulated Planetary Boundary Layer (PBL) height for  
199 Seville and Huelva shows that the majority of days in January 2013 had PBL values < 1000 m  
200 (Fig. 2g and h), while in June 2013 in Seville, the simulated daily peak PBL values were

201 between 1500 to 2750 m (Fig. 3g) with the majority of days having PBL values > 2000 m. In  
 202 Huelva in the summer period, the simulated PBL values were generally slightly lower than in  
 203 Seville, with daily peak values between 1060 to 2450 m (Fig. 3h) with the majority of days  
 204 having PBL values > 1500 m. It was not possible to compare the simulated PBL heights with  
 205 observational data, as there were no radio sounding data publicly available for any sites close  
 206 to or representative of Seville or Huelva during these periods.



207  
 208 Figure 3. Observed and simulated wind speed (a, b) and wind direction (c, d) at 10 m, temperature at 2 m (e, f)  
 209 and simulated PBL height (g, h) during June 2013 at Seville Tablada (left panel) and Ronda Este (right panel).  
 210

211 **Table 1.** Statistical metrics for observed and simulated meteorological variables at Seville  
 212 Tablada and Huelva Ronda Este sites.

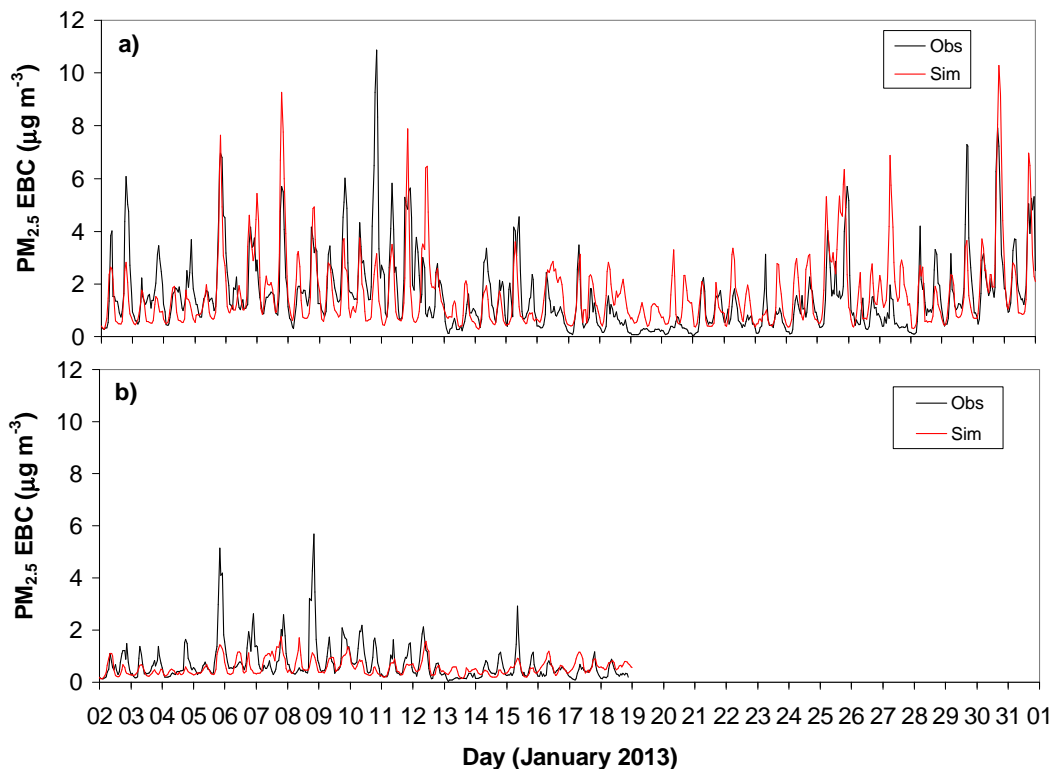
	SM	OM	MB	NMB (%)	R
<b>January 2013</b>					
WS, Seville Tablada ( $\text{m s}^{-1}$ )	2.7	1.5	1.1	72	0.75
T 2m, Seville Tablada ( $^{\circ}\text{C}$ )	10.4	10.8	-0.4	-3	0.91
WS, Huelva RE ( $\text{m s}^{-1}$ )	3.5	2.5	0.9	36	0.80
T 2m, Huelva RE ( $^{\circ}\text{C}$ )	11.1	11.4	-0.3	-3	0.90
<b>June 2013</b>					
WS, Seville Tablada ( $\text{m s}^{-1}$ )	2.8	1.7	1.1	64	0.57
T 2m, Seville Tablada ( $^{\circ}\text{C}$ )	24.3	24.2	0.2	1	0.95
WS, Huelva RE ( $\text{m s}^{-1}$ )	4.0	2.8	1.1	39	0.48
T 2m, Huelva RE ( $^{\circ}\text{C}$ )	22.9	22.5	0.4	2	0.95

213 WS (Wind speed at 10 m), T (Air temperature at 2 m), SM (Simulated mean), OM (Observed mean), MB (Mean Bias), NMB (Normalized  
 214 Mean Bias), R (Correlation Coefficient).  
 215



### 216 3.2 BC Seasonal and Day to Day Variation

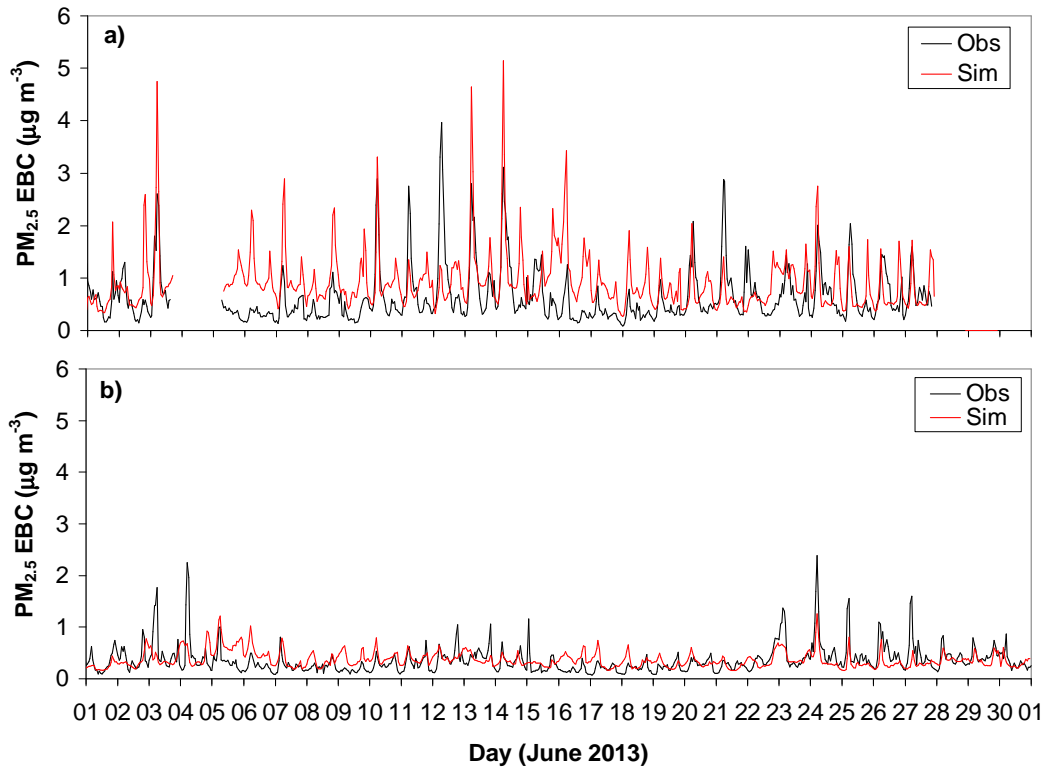
217 A large seasonal variation in EBC concentrations was observed at both sites, with maximum  
218 concentrations occurring in the winter period. The maximum observed hourly PM<sub>2.5</sub> EBC  
219 concentration at Príncipes, Seville for the winter and summer period were 10.9 µg m<sup>-3</sup> and  
220 4.0 µg m<sup>-3</sup>, respectively, with mean concentrations of 1.6 µg m<sup>-3</sup> and 0.6 µg m<sup>-3</sup> (Fig. 4a and  
221 5a). Observed PM<sub>2.5</sub> EBC concentrations were lower at University Campus, Huelva, with a  
222 mean and maximum of 0.7 µg m<sup>-3</sup> and 5.7 µg m<sup>-3</sup> in the winter period and 0.4 µg m<sup>-3</sup> and  
223 2.4 µg m<sup>-3</sup> in the summer period, respectively (Fig. 4b and 5b).



224  
225 Figure 4. Observed PM<sub>2.5</sub> EBC and simulated PM<sub>2.5</sub> PEC concentrations at a) Seville and b) Huelva, during  
226 January 2013. Observation data not available in Huelva for 19-31 Jan.

227 The modelling system performed generally well in capturing both these seasonal differences  
228 in concentration and the spatial variation between these two city sites. The EBC  
229 concentrations were slightly overestimated at the Seville site during winter (1.63 µg m<sup>-3</sup>  
230 simulated EBC versus 1.56 µg m<sup>-3</sup> measurements, MB = 0.07 µg m<sup>-3</sup>, NMB = 5%), while the  
231 EBC concentrations were underestimated during winter at the Huelva site (0.58 µg m<sup>-3</sup>  
232 simulated EBC versus 0.71 µg m<sup>-3</sup> measurements, MB = -0.14 µg m<sup>-3</sup>, NMB = -20%) (Table  
233 2). During the summer period, the EBC concentrations showed a greater overestimation at the

234 Seville site (MB = 0.29  $\mu\text{g m}^{-3}$ , NMB = 45%) while the mean bias was now slightly positive  
 235 for the Huelva site (MB = 0.01  $\mu\text{g m}^{-3}$ , NMB = 4%) (Table 2). Some of the discrepancy  
 236 between model and measurements in Huelva during the winter period could be attributed to  
 237 residential combustion emissions, which are not currently included in the emission inventory  
 238 in the inner domain. However, we would expect the contribution from this source sector to be  
 239 less in these urban areas than in rural areas and less in this southern Europe region in  
 240 comparison to northern Europe due to the warmer winter climate.



241  
 242 Figure 5. Observed  $\text{PM}_{2.5}$  EBC and simulated  $\text{PM}_{2.5}$  PEC concentrations at a) Seville and b) Huelva, during June  
 243 2013.

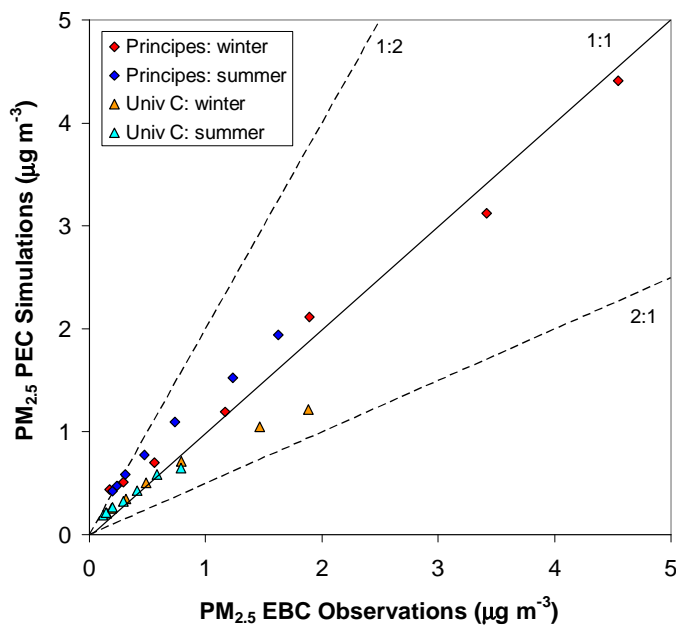
245 **Table 2.** Statistical metrics for observed EBC ( $\text{PM}_{2.5}$ ) and simulated  $\text{PM}_{2.5}$  PEC at Príncipes  
 246 (Seville) and University Campus (Huelva).

	SM ( $\mu\text{g m}^{-3}$ )	OM ( $\mu\text{g m}^{-3}$ )	MB ( $\mu\text{g m}^{-3}$ )	NMB (%)	R
<b>January 2013</b>					
Príncipes	1.63	1.56	0.07	5	0.60
University Campus	0.58	0.71	-0.14	-20	0.50
<b>June 2013</b>					
Príncipes	0.93	0.63	0.29	45	0.44
University Campus	0.37	0.35	0.01	4	0.37

247 SM (Simulated mean), OM (Observed mean), MB (Mean Bias), NMB (Normalized Mean Bias), R (Correlation Coefficient).

248 As well as capturing the seasonal variation, the model also captured the day to day variation  
249 within the months, for example capturing the peak concentrations observed at the Príncipes  
250 site on the 5, 7, 11 and 30 January 2013 as well as the lower concentrations observed on days  
251 such as the 13 and 19 January (Fig. 4a). However, as can be expected, there are some specific  
252 days where the modelling system does not capture peaks (e.g. 10 and 29 Jan, Príncipes or 5  
253 and 8 Jan, University Campus) and this is likely due to actual emission pattern changes from  
254 day to day that are not possible to capture in the model or deficiencies in the simulated  
255 meteorological fields for that day.

256 In general, the modelling system captured the large range observed in the hourly EBC  
257 concentrations ( $0.03 \mu\text{g m}^{-3}$  to  $10.9 \mu\text{g m}^{-3}$ ). This is demonstrated by the Q-Q plot for  
258 observed and simulated  $\text{PM}_{2.5}$  PEC concentrations (Fig. 6) which shows good agreement  
259 throughout the entire quantile range for the Príncipes site during the winter period, while  
260 demonstrating the overestimation of the quantiles in the summer period.  $\text{PM}_{2.5}$  PEC  
261 simulations at University Campus show the underestimation at the highest quantiles during  
262 the winter period and the reasonable agreement in the rest of the quantile range for both  
263 summer and winter periods (Fig. 6).



264  
265 Figure 6. Q-Q plot for simulated  $\text{PM}_{2.5}$  PEC concentrations versus  $\text{PM}_{2.5}$  EBC observations, 5th, 10th, 25th, 50th,  
266 75th, 90th and 95th percentiles are plotted for Príncipes and University Campus sites during winter (January  
267 2013) and summer (June 2013).

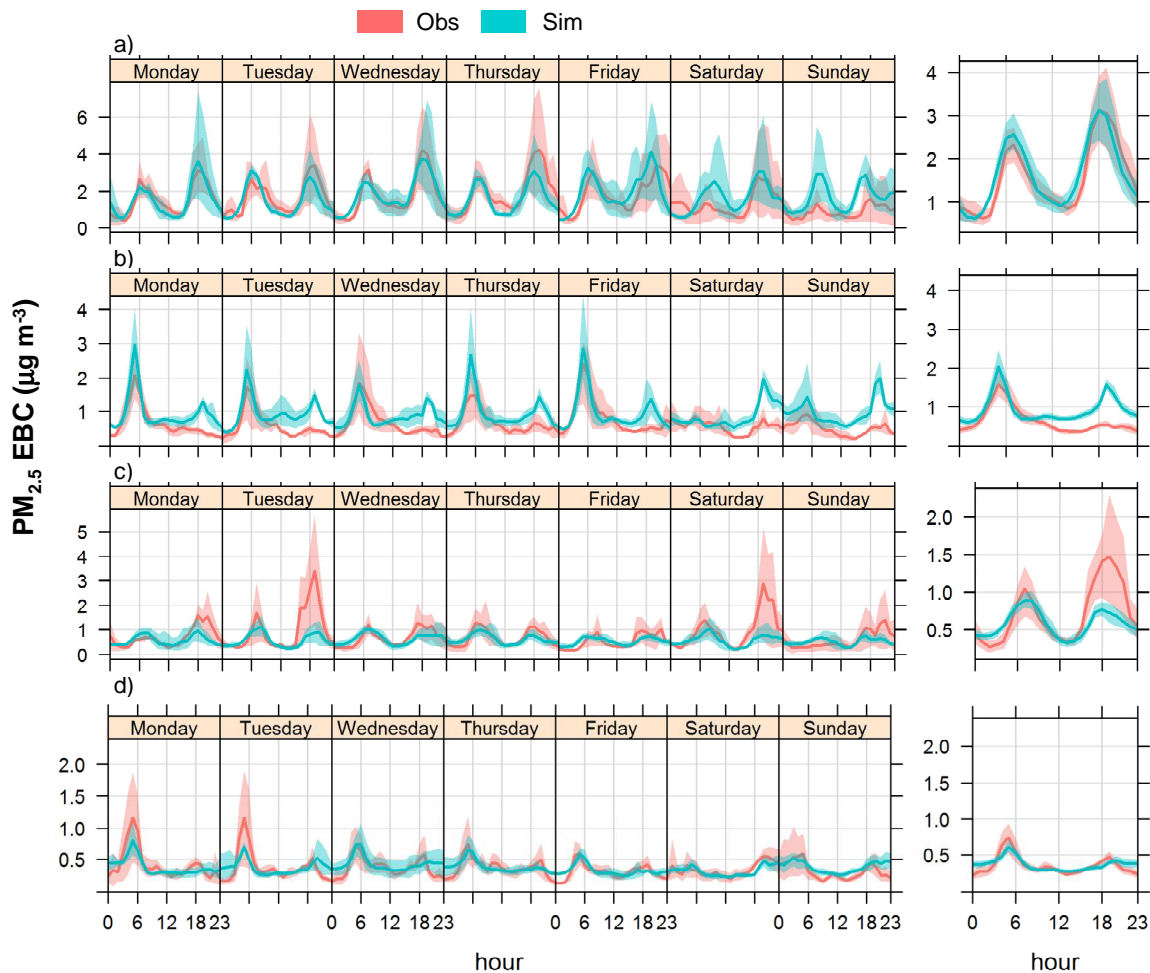
268 The emissions implemented in the modelling system do not vary seasonally; there is an hourly  
269 temporal profile used to disaggregate the on-road traffic emissions which differs for workdays  
270 and weekends (see section 2.3), but no seasonal variation. Therefore, the relatively close  
271 agreement of the model simulations with measurements supports the conclusion that, both the  
272 day to day variation and the seasonal variation in BC concentration in these urban areas in  
273 southern Spain are largely driven by the seasonal and day to day variation in meteorological  
274 conditions. This has been suggested by previous measurement studies (e.g. Pereira et al.,  
275 2012; Querol et al., 2013), but the modelling analysis confirms the driving role of the  
276 meteorology. Although the meteorology largely explains the relative distribution between  
277 winter and summer and the peaks, it is important to note that the total magnitude of  
278 concentrations is still driven by the emission strength.

### 279 **3.3 BC Diurnal Variation**

280 The high temporal resolution of the measurements allows the temporal variation during the  
281 day to be explored. The mean diurnal observed and simulated PM<sub>2.5</sub> PEC concentrations for  
282 each day of the week are shown in Fig. 7 for both sites for the winter and summer periods,  
283 along with the mean diurnal concentrations calculated for all data for each period. At the  
284 Príncipes site, during winter, the observed PM<sub>2.5</sub> EBC concentrations show a maximum in the  
285 morning between 06:00-08:00 UTC and then the concentrations decrease to reach a minimum  
286 at 14:00 (Fig. 7a). In the late afternoon/evening a secondary maximum is observed between  
287 17:00-19:00 UTC and the observed PM<sub>2.5</sub> EBC concentrations reach their highest values at  
288 this point. The simulated PM<sub>2.5</sub> PEC concentrations generally capture this winter diurnal  
289 variation well, with similar timing for the two peaks. However, the model overestimates the  
290 concentrations at the weekend, particularly on Sunday; this is likely due to an overestimation  
291 of the traffic emissions at the weekend.

292 In the summer period at the Príncipes site, it is interesting to note that the secondary  
293 maximum in the observed concentrations at 19:00 UTC is now very much smaller than the  
294 first maximum observed between 04:00-06:00 UTC and nearly non-existent (Fig. 7b). This  
295 marked change in the diurnal behaviour of EBC concentrations in the summer season,  
296 compared to the winter, has been observed in other studies (e.g. Saha and Despiiau, 2009).  
297 They measured BC over a 14-month period at an urban coastal location in south-east France,  
298 and found a similar disappearance of the secondary BC peak in the summer. Although the  
299 model does simulate a reduced secondary peak compared to the winter period, it doesn't

300 capture the near disappearance of the secondary peak (Fig 7b), which helps explain the poorer  
 301 correlation and greater positive bias seen in the performance of the model in the summer  
 302 (Table 2). Similarly to the winter period, there is a greater discrepancy between the model and  
 303 the measurements during the weekend, which suggests that the current traffic emission profile  
 304 overestimates weekend emissions.



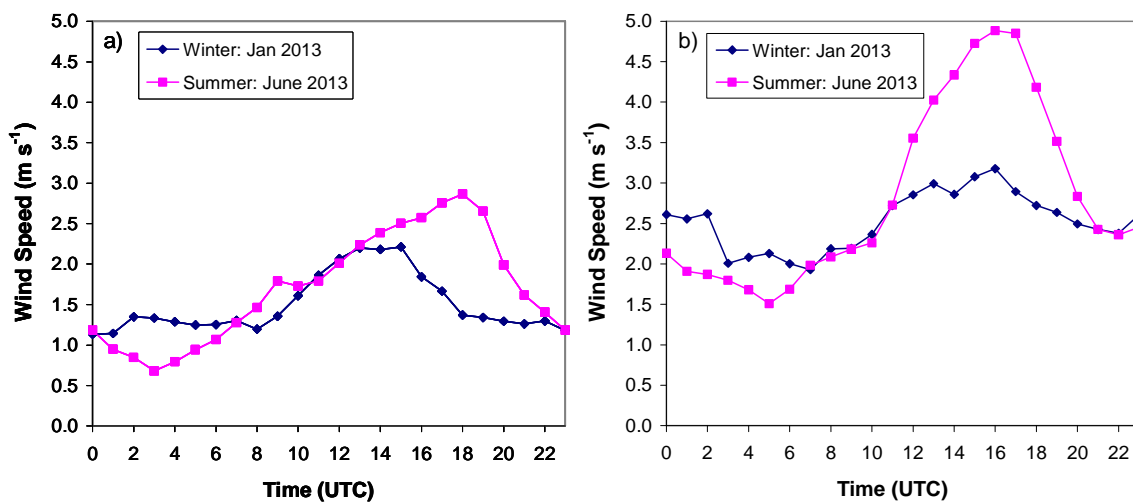
305  
 306 Figure 7. Mean diurnal observed PM<sub>2.5</sub> EBC and simulated PM<sub>2.5</sub> PEC concentrations for each day of the week  
 307 for Príncipe, Seville during a) January 2013 and b) June 2013 and at Univ Campus, Huelva, during c) January  
 308 2013 and d) June 2013. Also shown are the mean diurnals calculated for all data for each period in the right-hand  
 309 panel. Shaded areas represent 95% confidence interval in the mean. Graphics were generated with Openair  
 310 software (Carslaw and Ropkins, 2012).

311 At the University Campus site, during winter, the observed PM<sub>2.5</sub> EBC concentrations also  
 312 show a maximum in the morning between 06:00-08:00 UTC and a larger secondary  
 313 maximum occurring in the evening between 18:00-20:00 UTC (Fig. 7c). The model  
 314 simulations capture the timing of the peaks but underestimates the afternoon peak in the

315 observations. However, it should be noted that the afternoon peak in the observations shows a  
316 large variation in the mean, likely arising from peaks occurring on specific days (Fig. 7c).

317 During summer at the University Campus site the observed PM<sub>2.5</sub> EBC concentrations also  
318 show a maximum observed in the morning between 04:00-06:00 UTC and a much reduced  
319 secondary maximum in the evening between 18:00-20:00 UTC (Fig. 7d). The model captures  
320 this diurnal behaviour and in general, captures the magnitude of the concentrations.

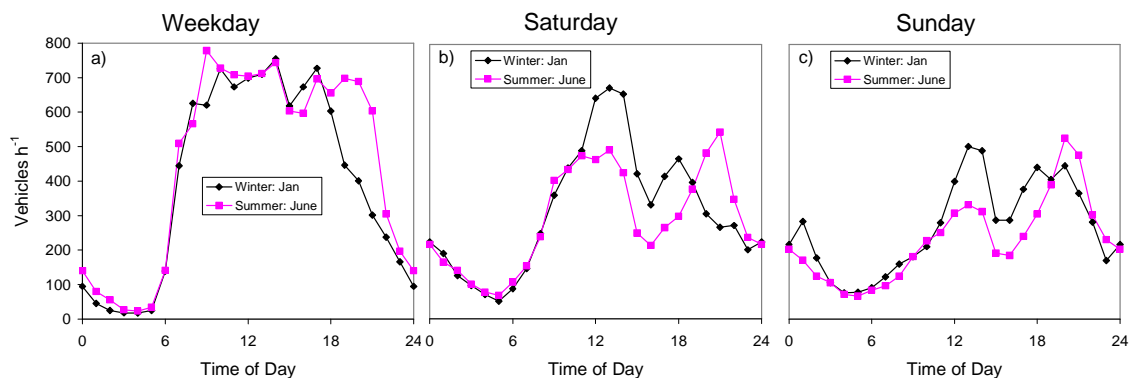
321 Saha and Despiau, (2009) propose that the appearance of the secondary maximum in winter,  
322 and the corresponding disappearance of the secondary maximum in summer, can likely be  
323 attributed to wind speed and boundary layer dynamics. A shallower boundary layer and lower  
324 wind speeds during winter will lead to higher concentrations, while the converse, higher wind  
325 speeds and a deeper boundary layer lasting for longer in the day during summer lead to  
326 reduced concentrations. The measurements and simulations performed here support these  
327 conclusions. The mean observed diurnal wind speed in Seville, Tablada (Fig. 8a) and Huelva,  
328 Ronda Este (Fig. 8b) both show a larger maximum in wind speeds in the summer with the  
329 maximum occurring later in summer and generally lasting longer, only returning to a  
330 minimum at about 22:00 UTC.



331  
332 Figure 8. Mean diurnal observed wind speed for a) Seville, Tablada and b) Huelva, Ronda Este during January  
333 2013 and June 2013.

334 In addition, road-traffic intensity data measurements from the main road closest to the  
335 Príncipes measurement site in Seville (Avenida de Blas Infante) demonstrate that there is very  
336 little seasonal variation in the weekday road-traffic intensity (Fig. 9a). The only significant  
337 seasonal difference is that the road-traffic intensity decreases later during the summer (~21.00

338 local time) compared to the winter (~18.00 local time) as can be expected due to extra  
 339 daylight hours in the summer. These measurements support the conclusions that the seasonal  
 340 variation in BC concentration in these urban areas in southern Spain is largely driven by the  
 341 seasonal variation in meteorology rather than a seasonal variation in emission strength.



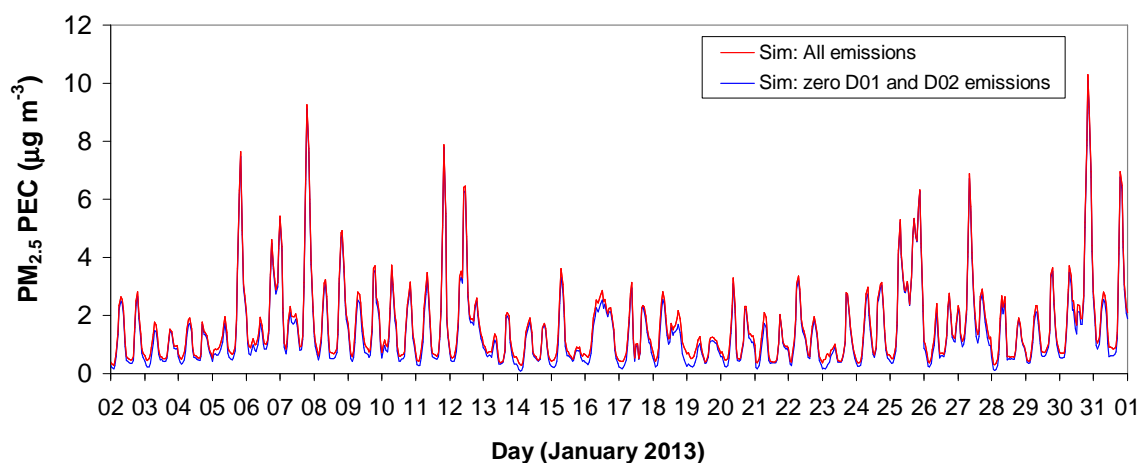
342  
 343 Figure 9. Mean diurnal road-traffic intensity (number of vehicles hour<sup>-1</sup>) for Seville (Blas Infante) for a)  
 344 Weekday, b) Saturday and c) Sunday during January 2013 and June 2013. Time is local time, UTC+1h in winter,  
 345 UTC+2 h in summer.

346 There are some small seasonal differences in the weekend road-traffic intensity (Fig. 9b and  
 347 c). The total vehicle counts are similar for January and June but the diurnal behaviour is  
 348 different. In winter, the first peak in road-traffic intensity is larger than the second peak  
 349 whereas the converse is true in the summer. This increase in road-traffic intensity in the  
 350 evening peak with respect to the morning peak in summer is in contrast to the near  
 351 disappearance of the secondary peak in EBC concentrations in the summer, therefore also  
 352 providing evidence that the reduction of the secondary peak in EBC concentrations in the  
 353 summer is dominated by meteorological processes not emission changes.

### 354 3.4 Evaluation of regional and local contribution to BC concentrations

355 In order to evaluate the role of regional transport of BC in this study area, the modelling  
 356 system was used to compare the base case emission scenario, with all emissions included in  
 357 all three modelling domains (denoted “all emissions”) with a scenario in which the emissions  
 358 in the outer two domains were set to zero (denoted “zero D01 and D02 emissions”). As  
 359 described in Section 2.2, domain D01 covers the Iberian Peninsula, and parts of southern  
 360 France and North Africa while domain D02 includes parts of southern Spain and southern  
 361 Portugal. For the sake of brevity, the scenario results are only shown for the Príncipes site in  
 362 January 2013 (Fig. 10).

363



364  
 365 Figure 10. Simulated PM<sub>2.5</sub> PEC concentration ( $\mu\text{g m}^{-3}$ ) for the base case emission scenario (All emissions) and  
 366 the zero D01 and D02 emissions scenario, for Príncipes measurement site, Seville during January 2013.

367 We observe that the simulated EBC concentrations only decrease slightly, with respect to the  
 368 base case scenario, when we remove the outer domain emissions (Fig. 10). The mean relative  
 369 changes in the simulated PM<sub>2.5</sub> EBC concentration for the Príncipes site during January and  
 370 June 2013 were -16% and -17%, respectively, while the mean absolute changes in the  
 371 simulated PM<sub>2.5</sub> EBC concentration were  $-0.17 \mu\text{g m}^{-3}$  and  $-0.14 \mu\text{g m}^{-3}$ , respectively. This  
 372 indicates that regional transport of BC is not a large contributor to EBC concentrations in the  
 373 medium size urban area of Seville and local sources are dominant.

374 The mean absolute changes in simulated PM<sub>2.5</sub> EBC concentration for the Huelva site during  
 375 January and June 2013 were  $-0.19 \mu\text{g m}^{-3}$  and  $-0.18 \mu\text{g m}^{-3}$ , respectively. These absolute  
 376 values in Huelva were similar to those in Seville. However, as the overall magnitude of EBC  
 377 concentrations was less in Huelva, the relative percentage contribution of the regional  
 378 transport of BC was larger. The mean relative changes in the simulated PM<sub>2.5</sub> EBC  
 379 concentration, with respect to the base case scenario, when we remove the outer domain  
 380 emissions for the Huelva site during January and June 2013 were -37% and -46%,  
 381 respectively. Therefore, in the small size city of Huelva, regional sources potentially provide a  
 382 contribution to EBC concentrations similar to that of local sources.

#### 383 4 Conclusions

384 A measurement and modelling program has been initiated in south-west Spain to characterise  
 385 the concentrations and behaviour of black carbon in two different cities. A large seasonal  
 386 variability was observed in PM<sub>2.5</sub> EBC concentration in the two cities, with higher



387 concentrations in wintertime. The summertime EBC concentrations were typically less than  
388 half those of the wintertime.

389 The modelling system reproduces the diurnal, seasonal and day to day variation in EBC  
390 concentrations, with mean biases at the two sites in the winter and summer period ranging  
391 from -0.14 to 0.29  $\mu\text{g m}^{-3}$ . Although there are some specific days where the modelling system  
392 does not capture peaks, in general the large range observed in the hourly EBC concentrations  
393 is reproduced. This suggests that the system is capturing the dominant processes that affect  
394 the EBC concentrations in these urban areas, namely the meteorology and the spatial and  
395 temporal distribution of emissions.

396 The modelling analysis demonstrates that the seasonal variation in EBC concentration in these  
397 urban areas in southern Spain is largely driven by the seasonal variation in meteorology, with  
398 reduced dispersion conditions in wintertime leading to higher concentrations. There is little  
399 seasonal variation in emission strength as also demonstrated by road traffic intensity  
400 measurements near the Seville site. There is a large day to day variation in EBC concentration  
401 observed within both the winter and summer months, with more than an order of magnitude  
402 difference between the highest (3.4  $\mu\text{g m}^{-3}$ ) and lowest (0.2  $\mu\text{g m}^{-3}$ ) mean daily concentrations  
403 at the Príncipes Seville site, during January 2013, for example. This day to day variability also  
404 seems to be primarily driven by the variation in meteorological conditions, along with some  
405 contribution from the differences in emission intensities between weekday and weekend days.  
406 It is important to note that although the meteorological conditions largely explain the relative  
407 distribution between winter and summer and the peaks on different days, the total magnitude  
408 of concentrations is still driven by emission strength.

409 The high temporal resolution in the measurements aids the understanding of the diurnal  
410 variability of EBC concentrations and demonstrates that the diurnal variation of EBC in these  
411 urban areas is bimodal, with a morning and evening peak. However, there was a marked  
412 seasonality in the diurnal pattern, with the EBC evening peak being larger than the morning  
413 peak in the wintertime, while nearly disappearing in the summertime. This is consistent with a  
414 deeper boundary layer lasting for longer in the day during summer reducing EBC  
415 concentrations. Although the model does simulate a reduced secondary peak compared to the  
416 winter period, it doesn't fully simulate the near disappearance of the secondary peak which  
417 helps explain the larger discrepancy between the model and measurements observed during  
418 the summer period at the Seville site. The comparison between model and measurements also

419 indicates that the profile utilised for the temporal disaggregation of the road traffic emissions  
420 during the weekend is likely overestimating the weekend emissions and future work will  
421 enable an improvement in these temporal profiles.

422 An evaluation of the role of regional transport of BC in this study area, comparing scenarios  
423 with and without outer domain emissions, demonstrated that regional transport of BC is not a  
424 large contributor to EBC concentrations in a medium sized urban area, such as Seville, and  
425 local sources, such as on-road traffic emissions, are dominant. However, in a small sized city,  
426 such as Huelva, local sources play a less dominant role and the regional contribution is  
427 potentially similar to that of local sources. The contribution from residential combustion,  
428 which is not present in the emission inventory, is considered to be minor. However, it could  
429 contribute to the underestimation of EBC concentrations observed in Huelva in the winter  
430 period and future improvements to our modelling system would include the implementation  
431 of this emission source.

432 It has been suggested that diesel sources provide the most promising black carbon mitigation  
433 options (Bond et al., 2013) and we conclude that reduction of BC from diesel on-road sources  
434 in these urban areas would indeed be a way forward to gain maximum benefits in both climate  
435 mitigation and air quality and resulting health benefit. Based on the results here, we propose  
436 that mitigation strategies aimed at a targeted control, for example reducing the heaviest on-  
437 road emitters in wintertime, would yield the greatest benefits.

438 The issue of reduction of on-road diesel BC emissions is particularly relevant for Spain as it is  
439 one of the countries in Europe which has experienced the largest dieselisation of its vehicle  
440 fleet in recent years. Its percentage share of diesel cars in its total passenger car fleet rose  
441 from 15% in 1995 to 50% in 2009, placing it 5<sup>th</sup> out of the 30 EEA member countries (EEA,  
442 2011) in terms of its diesel share and substantially greater than the EEA average of 28%. The  
443 diesel percentage share of the total passenger car fleet and indeed of the total vehicle fleet has  
444 continued to rise in Spain, to 55% and 56% in 2013 (DGT, 2013). Taking into account that  
445 BC has been identified as a more sensitive indicator to vehicle exhaust related air pollution,  
446 the parallel measurement and modelling of BC in urban areas constitutes a useful tool to both  
447 evaluate the potential of any proposed traffic emission reduction measures while also  
448 monitoring the effectiveness of any traffic emission reduction measures already implemented.

449

450

## 451 Acknowledgements

452 The authors gratefully acknowledge funding from the Department of Innovation, Science and  
453 Enterprise of the Government of Andalusia through the research projects SIMAND (P07-  
454 RNM-02729) and (2011RNM-7800) and from the Department of Environment, Andalusian  
455 Regional Government (project: 199/2011/C/00). In addition, we thank the Spanish Ministry of  
456 Economy and Competitiveness for funding through the project POLLINDUST (CGL2011-  
457 26259). We would also like to thank the Government of Andalusia for providing data from  
458 their Air Quality Network and from their Atmospheric Emissions Inventory and AEMET for  
459 providing meteorological data. We also thank Dr. Fantine Ngan for providing the GEOS-  
460 Chem data.

## 461 References

- 462 Barrett, S.R.H., Yim, S.H.L., Gilmore, C.K., Murray, L.T., Kuhn, S.R., Tai, A.P.K., Yantosca, R.M., Byun,  
463 D.W., Ngan, F., Li, X., Levy, J.I., Ashok, A., Koo, J., Wong, H.M., Dessens, O., Balasubramanian, S.,  
464 Fleming, G.G., Pearlson, M.N., Wollersheim, C., Malina, R., Arunachalam, S., Binkowski, F.S.,  
465 Leibensperger, E.M., Jacob, D.J., Hileman, J.I., Waitz, I.A., 2012. Public health, climate, and economic  
466 impacts of desulfurizing jet fuel. *Environ. Sci. Technol.* 46, 4275–82.
- 467 Bey, I., Jacob, D.J., Yantosca, R.M., Logan, J.A., Field, B.D., Fiore, A.M., Li, Q., Liu, H.Y., Mickley, L.J.,  
468 Schultz, M.G., 2001. Global modeling of tropospheric chemistry with assimilated meteorology: Model  
469 description and evaluation. *J. Geophys. Res.* 106, 23073. doi:10.1029/2001JD000807
- 470 Bond, T.C., Doherty, S.J., Fahey, D.W., Forster, P.M., Bernsten, T., DeAngelo, B.J., Flanner, M.G., Ghan, S.,  
471 Kärcher, B., Koch, D., Kinne, S., Kondo, Y., Quinn, P.K., Sarofim, M.C., Schultz, M.G., Schulz, M.,  
472 Venkataraman, C., Zhang, H., Zhang, S., Bellouin, N., Guttikunda, S.K., Hopke, P.K., Jacobson, M.Z.,  
473 Kaiser, J.W., Klimont, Z., Lohmann, U., Schwarz, J.P., Shindell, D., Storelvmo, T., Warren, S.G.,  
474 Zender, C.S., 2013. Bounding the role of black carbon in the climate system: A scientific assessment. *J.*  
475 *Geophys. Res. Atmos.* 118, 5380–5552. doi:10.1002/jgrd.50171
- 476 Brook, R.D., Rajagopalan, S., Pope, C.A., Brook, J.R., Bhatnagar, A., Diez-Roux, A. V., Holguin, F., Hong, Y.,  
477 Luepker, R. V., Mittleman, M.A., Peters, A., Siscovick, D., Smith, S.C., Whitsel, L., Kaufman, J.D.,  
478 2010. Particulate matter air pollution and cardiovascular disease: An update to the scientific statement  
479 from the American Heart Association. *Circulation* 121, 2331–78.
- 480 Carslaw, D.C., Ropkins, K., 2012. openair — An R package for air quality data analysis. *Environ. Model. Softw.*  
481 27–28, 52–61. doi:10.1016/j.envsoft.2011.09.008
- 482 Castell, N., Mantilla, E., Salvador, R., Stein, A.F., Millán, M., 2010. Photochemical model evaluation of the  
483 surface ozone impact of a power plant in a heavily industrialized area of southwestern Spain. *J. Environ.*  
484 *Manage.* 91, 662–76.
- 485 Cavalli, F., Viana, M., Yttri, K.E., Genberg, J., Putaud, J.-P., 2010. Toward a standardised thermal-optical  
486 protocol for measuring atmospheric organic and elemental carbon: the EUSAAR protocol. *Atmos. Meas.*  
487 *Tech.* 3, 79–89.
- 488 CEIDARS, 2012. Particle size fraction data for source categories. California Emission Inventory and Reporting  
489 System, California Environmental Protection Agency, Air Resources Board, Sacramento, California.
- 490 Couvidat, F., Kim, Y., Sartelet, K., Seigneur, C., Marchand, N., Sciare, J., 2013. Modeling secondary organic  
491 aerosol in an urban area: application to Paris, France. *Atmos. Chem. Phys.* 13, 983–996.
- 492 DGT, 2013. Anuario Estadístico General. Año 2013. Dirección General de Tráfico, Ministerio del Interior,  
493 Madrid, Spain.
- 494 EEA, 2011. Dieselisation in the EEA. European Environment Agency, Copenhagen, Denmark,  
495 <http://www.eea.europa.eu/data-and-maps/figures/dieselisation-in-the-eea>, Accessed 1/10/2014.
- 496 EEA, 2013. Status of black carbon monitoring in ambient air in Europe, EEA Technical report, No 18/2013.  
497 European Environment Agency, Copenhagen, Denmark, 43pp, doi:10.2800/10150.
- 498 Ensberg, J.J., Craven, J.S., Metcalf, A.R., Allan, J.D., Angevine, W.M., Bahreini, R., Brioude, J., Cai, C., Coe,  
499 H., de Gouw, J.A., Ellis, R.A., Flynn, J.H., Haman, C.L., Hayes, P.L., Jimenez, J.L., Lefer, B.L.,

500 Middlebrook, A.M., Murphy, J.G., Neuman, J.A., Nowak, J.B., Roberts, J.M., Stutz, J., Taylor, J.W.,  
501 Veres, P.R., Walker, J.M., Seinfeld, J.H., 2013. Inorganic and black carbon aerosols in the Los Angeles  
502 Basin during CalNex. *J. Geophys. Res. Atmos.* 118, 1777–1803. doi:10.1029/2012JD018136  
503 ENVIRON, 2008. Comprehensive Air Quality Model with Extensions (CAMx) Version 4.5. User’s Guide.  
504 ENVIRON International Corporation.  
505 EPA, 2009. Speciation Profile Usage Memorandum. US Environmental Protection Agency.  
506 Fernández-Camacho, R., Rodríguez, S., de la Rosa, J., Sánchez de la Campa, A.M., Viana, M., Alastuey, A.,  
507 Querol, X., 2010. Ultrafine particle formation in the inland sea breeze airflow in Southwest Europe.  
508 *Atmos. Chem. Phys.* 10, 9615–9630.  
509 GAW/WMO, 2011. Position of the GAW Scientific Advisory Group on the use of Black Carbon terminology.  
510 GAW/WMO SAG AEROSOLS.  
511 Genberg, J., Denier van der Gon, H.A.C., Simpson, D., Swietlicki, E., Areskoug, H., Beddows, D., Ceburnis, D.,  
512 Fiebig, M., Hansson, H.C., Harrison, R.M., Jennings, S.G., Saarikoski, S., Spindler, G., Visschedijk,  
513 A.J.H., Wiedensohler, A., Yttri, K.E., Bergström, R., 2013. Light-absorbing carbon in Europe –  
514 measurement and modelling, with a focus on residential wood combustion emissions. *Atmos. Chem.*  
515 *Phys.* 13, 8719–8738.  
516 Gilardoni, S., Vignati, E., Wilson, J., 2011. Using measurements for evaluation of black carbon modeling.  
517 *Atmos. Chem. Phys.* 11, 439–455.  
518 Grell, G.A., Dudhia, J., Stauffer, D.R., 1995. A Description of the Fifth-generation Penn State/NCAR Mesoscale  
519 Model (MM5). Tech. Rep. NCAR/TN-398+STR. National Center of Atmospheric Research (NCAR),  
520 USA.  
521 Hienola, A.I., Pietikäinen, J.-P., Jacob, D., Pozdun, R., Petäjä, T., Hyvärinen, A.-P., Sogacheva, L., Kerminen,  
522 V.-M., Kulmala, M., Laaksonen, A., 2013. Black carbon concentration and deposition estimations in  
523 Finland by the regional aerosol–climate model REMO-HAM. *Atmos. Chem. Phys.* 13, 4033–4055.  
524 IARC, 2012. Diesel Engine Exhaust Carcinogenic. International Agency for Research on Cancer, World Health  
525 Organization, Press Release No. 213, June 12, 2012, Accessed at [http://www.iarc.fr/en/media-](http://www.iarc.fr/en/media-centre/pr/2012/pdfs/pr213_E.pdf)  
526 [centre/pr/2012/pdfs/pr213\\_E.pdf](http://www.iarc.fr/en/media-centre/pr/2012/pdfs/pr213_E.pdf) on September 18, 2014.  
527 Janssen, N.A.H., Hoek, G., Simic-lawson, M., Fischer, P., Bree, L. Van, Brink, H., Keuken, M., Atkinson, R.W.,  
528 Anderson, H.R., Brunekreef, B., Cassee, F.R., 2011. Black Carbon as an Additional Indicator of the  
529 Adverse Health Effects of Airborne Particles Compared with PM<sub>10</sub> and PM<sub>2.5</sub>. *Environ. Health Perspect.*  
530 119, 1691–1699.  
531 Keuken, M.P., Jonkers, S., Zandveld, P., Voogt, M., Elshout van den, S., 2012. Elemental carbon as an indicator  
532 for evaluating the impact of traffic measures on air quality and health. *Atmos. Environ.* 61, 1–8.  
533 Keuken, M.P., Zandveld, P., Jonkers, S., Moerman, M., Jedynska, A.D., Verbeek, R., Visschedijk, A., Elshout  
534 van den, S., Panteliadis, P., Velders, G.J.M., 2013. Modelling elemental carbon at regional, urban and  
535 traffic locations in The Netherlands. *Atmos. Environ.* 73, 73–80.  
536 Koch, D., Schulz, M., Kinne, S., Mcnaughton, C., Spackman, J.R., Balkanski, Y., Bauer, S., Berntsen, T., 2009.  
537 Evaluation of black carbon estimations in global aerosol models. *Atmos. Chem. Phys.* 9001–9026.  
538 Lepeule, J., Laden, F., Dockery, D., Schwartz, J., 2012. Chronic exposure to fine particles and mortality: an  
539 extended follow-up of the Harvard Six Cities study from 1974 to 2009. *Environ. Health Perspect.* 120,  
540 965–70.  
541 Milford, C., Castell, N., Marrero, C., Rodríguez, S., Sánchez de la Campa, A.M., Fernández-Camacho, R., de la  
542 Rosa, J., Stein, A.F., 2013. Measurements and simulation of speciated PM<sub>2.5</sub> in south-west Europe.  
543 *Atmos. Environ.* 77, 36–50.  
544 Pereira, S.N., Wagner, F., Silva, A.M., 2012. Long term black carbon measurements in the southwestern Iberia  
545 Peninsula. *Atmos. Environ.* 57, 63–71.  
546 Petzold, A., Ogren, J.A., Fiebig, M., Laj, P., Li, S.-M., Baltensperger, U., Holzer-Popp, T., Kinne, S.,  
547 Pappalardo, G., Sugimoto, N., Wehrli, C., Wiedensohler, A., Zhang, X.-Y., 2013. Recommendations for  
548 reporting “black carbon” measurements. *Atmos. Chem. Phys.* 13, 8365–8379.  
549 Pope, C.A., Ezzati, M., Dockery, D.W., 2009. Fine-particulate air pollution and life expectancy in the United  
550 States. *N. Engl. J. Med.* 360, 376–386.  
551 Querol, X., Alastuey, A., Viana, M., Moreno, T., Reche, C., Minguillón, M.C., Ripoll, A., Pandolfi, M., Amato,  
552 F., Karanasiou, A., Pérez, N., Pey, J., Cusack, M., Vázquez, R., Plana, F., Dall’Osto, M., de la Rosa, J.,  
553 Sánchez de la Campa, A., Fernández-Camacho, R., Rodríguez, S., Pio, C., Alados-Arboledas, L., Titos,  
554 G., Artíñano, B., Salvador, P., García Dos Santos, S., Fernández Patier, R., 2013. Variability of  
555 carbonaceous aerosols in remote, rural, urban and industrial environments in Spain: implications for air  
556 quality policy. *Atmos. Chem. Phys.* 13, 6185–6206.  
557 Reche, C., Querol, X., Alastuey, A., Viana, M., Pey, J., Moreno, T., Rodríguez, S., González, Y., Fernández-  
558 Camacho, R., de la Rosa, J., Dall’Osto, M., Prévôt, A.S.H., Hueglin, C., Harrison, R.M., Quincey, P.,

559 2011. New considerations for PM, Black Carbon and particle number concentration for air quality  
560 monitoring across different European cities. *Atmos. Chem. Phys.* 11, 6207–6227.

561 Saha, A., Despiiau, S., 2009. Seasonal and diurnal variations of black carbon aerosols over a Mediterranean  
562 coastal zone. *Atmos. Res.* 92, 27–41.

563 Schaap, M., Denier van der Gon, H.A.C, Dentener, F.J., Visschedijk, A.J.H., van Loon, M., ten Brink, H. M.,  
564 Putaud, J.-P., Guillaume, B., Liousse, C., Builtjes, P.J.H., 2004. Anthropogenic black carbon and fine  
565 aerosol distribution over Europe. *J. Geophys. Res.* 109, D18207. doi:10.1029/2003JD004330

566 Sciare, J., D’Argouges, O., Zhang, Q.J., Sarda-Estève, R., Gaimoz, C., Gros, V., Beekmann, M., Sanchez, O.,  
567 2010. Comparison between simulated and observed chemical composition of fine aerosols in Paris  
568 (France) during springtime: contribution of regional versus continental emissions. *Atmos. Chem. Phys.*  
569 10, 11987–12004.

570 Simpson, D., Yttri, K.E., Klimont, Z., Kupiainen, K., Caseiro, A., Gelencsér, A., Pio, C., Puxbaum, H., Legrand,  
571 M., 2007. Modeling carbonaceous aerosol over Europe: Analysis of the CARBOSOL and EMEP EC/OC  
572 campaigns. *J. Geophys. Res.* 112, D23S14. doi:10.1029/2006JD008158

573 Tsyro, S., Simpson, D., Tarrasón, L., Klimont, Z., Kupiainen, K., Pio, C., Yttri, K.E., 2007. Modeling of  
574 elemental carbon over Europe. *J. Geophys. Res.* 112, D23S19. doi:10.1029/2006JD008164

575 UNEP, 2011. Near-term Climate Protection and Clean Air Benefits: Actions for Controlling Short-Lived  
576 Climate Forcers. United Nations Environment Programme (UNEP), Nairobi, Kenya, 78pp.

577 WHO, 2012. Health effects of black carbon, Janssen, N. A. H., Gerlofs-Nijland, M. E., Lanki, T., Salonen, R. O.,  
578 Cassee, F., Hoek, G., Fischer, P., Brunekreef, B., and Krzyzanowski, M. World Health Organization,  
579 Regional Office for Europe, Copenhagen, 86pp.

580 WHO, 2013. Review of evidence on health aspects of air pollution – REVIHAAP Project. World Health  
581 Organization, Regional Office for Europe, Copenhagen, 302pp.

582